Available online at www.sciencedirect.com
ScienceDirect
Journal of Power Sources 161 (2006) 115–122
JOURNAL OF POWER SOURCES
www.elsevier.com/locate/jpowsour

Performance of a novel La(Sr)Fe(Co)O_3–Ag SOFC cathode

Steven P. Simner*, Michael D. Anderson, James E. Coleman, Jeffry W. Stevenson

Pacific Northwest National Laboratory, Materials Science Division, Richland, WA 99352, United States

Received 14 March 2006; received in revised form 19 April 2006; accepted 20 April 2006
Available online 8 June 2006

Abstract

Atomized silver spheres (≤53 μm diameter) were coated with a 1 μm thick layer of $(La_{0.6}Sr_{0.4})_{0.98}Co_{0.2}Fe_{0.8}O_{3-\delta}$ via a mechanofusion dry processing method. The material was successfully utilized as an SOFC cathode on anode-supported YSZ electrolytes at 700 °C, producing >500 mW cm^{-2} (at 0.7 V) and exhibiting relatively stable performance (∼3% power degradation per 1000 h at 0.7 V) during >2000 h of operation.

Keywords: SOFC; Cathode; Silver; LSCF

1. Introduction

Conductive oxides, such as La(Sr)MnO_3, La(Sr)CoO_3, La(Sr)FeO_3, and La(Sr)Fe(Co)O_3, mixed with noble metals, including palladium, platinum and silver (typically < 5 wt.%), have been the subject of numerous SOFC-related studies due to their increased activity towards oxygen reduction [1–14]. Such materials have typically been produced in one of five ways: (1) mixing noble metal precursor solutions with cathode nitrate solutions (e.g. Pt diamine nitrite added to La–Sr–Fe nitrate solution, i.e. $La(NO_3)_3$, $Sr(NO_3)_2$, $Fe(NO_3)_3$) to produce an intimate mixture of noble metal/cathode powder after combustion synthesis [1,2], (2) mixing cathode oxide powders with noble metal powders prior to application and sintering [1,3–5], (3) dual sputtering of oxide and noble metal from separate sputtering targets [6], (4) application of noble metal containing precursor solutions to the electrolyte surface prior to cathode application and firing [7,8], and (5) impregnation of precursor solutions after cathode sintering [9–14]. Whilst these additions provide well documented improvements in cathode activity, the Pd and Pt based composites materials can be cost-prohibitive due to the raw material expense. Silver is, of course, a more affordable option though the low melting point of Ag (962 °C) and diffusivity/volatility at current SOFC operating temperatures (700–800 °C) are considered problematic. A good review of studies involving the addition of noble metals to SOFC cathodes is presented in a recent article by Haanappel et al. [15].

The work presented in this article describes a novel oxide–Ag composite morphology. The originally intended application of the material was as a contact paste between SOFC cathodes and metal alloy interconnects, but somewhat unexpectedly the composite has also shown promise when used directly as an SOFC cathode. The composite in this particular study consists of silver spherical cores up to 53 μm diameter coated with a 1 μm layer of $(La_{0.6}Sr_{0.4})_{0.98}Fe_{0.8}Co_{0.2}O_3$ (LSCF-6428) cathode powder. The primary purpose for applying the oxide coating was the reduction of silver diffusivity and/or volatility. The composite is formed via a dry coating technique known as "mechanofusion". Pre-determined proportions of the silver spheres (termed the host particles), and sub-micron ceramic oxide powders (guest particles) are mixed under high shear and compressive forces. The forces are capable of embedding the oxide powders into the ductile Ag host without drastically changing the original shape of the host material. In addition, the heat generated from these forces can have the added benefit of fusing the guest particles to the host. The mechanofusion process will not be considered in depth within this article, but a good review of mechanofusion and other similar dry coating techniques is presented by Pfeffer et al. [17].

The use of dry particle coating technologies to coat ductile metal spheres with oxide powders is not new, and has been successfully implemented for coating copper spheres (∼70 μm diameter) with sub-micron alumina particles in order to increase

* Corresponding author.
E-mail address: Steven.Simner@pnl.gov (S.P. Simner).

0378-7753/$ – see front matter © 2006 Elsevier B.V. All rights reserved.
doi:10.1016/j.jpowsour.2006.04.103

the surface hardness of the Cu [18]. In addition, the method has also been considered for processing fuel cell materials including NiO-YSZ SOFC anode composites [19], and CoO/Ni and $MgFe_2O_4$/Ni for molten carbonate fuel cell (MCFC) cathodes [20]. In the former case, 2–10 μm NiO (not metallic Ni) particles were processed with sub-micron YSZ powders, and for the latter study Ni filaments (∼3 μm) were coated with sub-micron CoO or $MgFe_2O_4$ particles.

2. Experimental

Anode-supported electrolyte (8YSZ) membranes (1 mm thickness, 25 mm diameter) were produced via standard organic tape-casting and tape lamination procedures, co-sintered at 1375 °C for 1 h, and subsequently creep-flattened at 1350 °C for 2 h. $(La_{0.6}Sr_{0.4})_{0.98}Fe_{0.8}Co_{0.2}O_3$ (LSCF-6428) cathode and $Ce_{0.8}Sm_{0.2}O_{1.9}$ (SDC-20) interlayer powders were supplied by Praxair Specialty Ceramics, Seattle, WA. Atomized silver spheres were purchased from Technic Inc. (Engineered Powders Division), Woonsocker, RI. The size range of the spheres was −270/+325 mesh (53–44 μm particle sizes) though as indicated by Fig. 1 smaller particles were also retained within the powder. LSCF–Ag composites (∼5 wt.% LSCF) were produced via a mechanofusion technique using a Hosokawa Mechanofusion System AMS-Mini. Processing and subsequent microstructural optimization, with respect to maximizing surface coverage, was performed by Hosokawa Micron Powder Systems, Summit, NJ, and is not the subject of this particular study. SDC-20 interlayers (∼5 μm sintered thickness) were applied to the anode-supported YSZ membranes via screen-printing, and sintered at 1200 °C for 2 h; the sintered SDC layers contained ∼25–35% porosity. Such layers are typically used to prevent interaction between the cathode and the YSZ electrolyte resulting in the formation of interfacial and resistive La- and or Sr-zirconate phases. Anode current collectors (Ni mesh embedded in NiO paste) were co-sintered with the ceria. Cathode compositions were applied by screen-printing (1.6 cm diameter print – 2 cm^2), and then sintered in situ during heat up (and sealing) of the cell to 800 °C. The

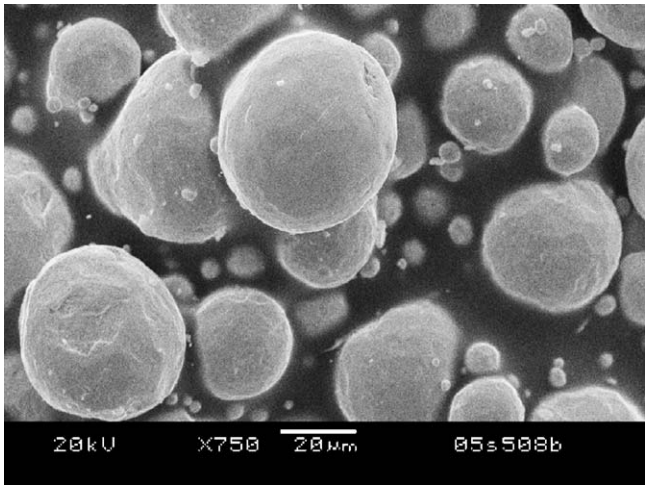

Fig. 1. Commercially supplied silver spheres (44–53 μm diameter) with retained fines.

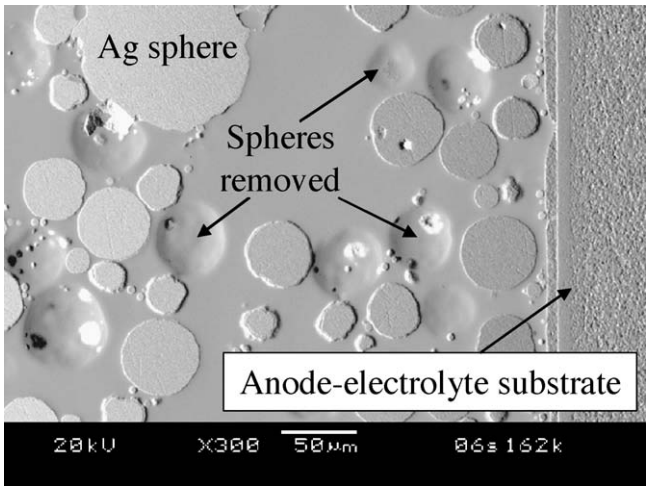

Fig. 2. Topographic image indicating severe particle pull-out during SEM sample preparation.

cathode area was used as the active cell area to calculate power density and area specific resistance. A combination of gold mesh and foil were used as the cathode current collector, and simply pressed into the wet cathode ink prior to heat up. The cells were sealed to alumina test fixtures using Aremco cements (sintered at 800 °C/1 h), and compressive stress (∼10 psi) applied to the cell via a perforated alumina stub spring loaded outside the furnace hot zone (detailed in [21]).

Current–voltage (*I–V*) and electrochemical impedance (EIS) data was recorded at 700–750 °C using a Solartron 1480 Multistat and 1255 Frequency Response Analyzer. Cells were held at 0.7 V for 250–2000+ h and subjected to impedance measurements every 24–50 h. A 250 mA dc bias was applied to the cells for EIS measurements, and data recorded from 2 MHz to 0.1 Hz with a 100 mA amplitude. 48.5% H_2–48.5% N_2–3% H_2O was flowed to the anode at 200 sccm, and air to the cathode at 200 sccm (ambient air relative humidity was approximately 35–45%). Room temperature X-ray diffraction (XRD) analysis of reacted LSCF-6428/8-YSZ powder mixtures was obtained (0.02° step size and 1 s hold time) using a Philips Wide-Range Vertical Goniometer and a Philips XRG3100 X-ray Generator. SEM/EDX was conducted with a JEOL JSM-5900LV microscope with an OXFORD Instruments INCA Energy 200 X-ray detector. A point to note with respect to preparation of samples for SEM. Samples were initially potted with epoxy (under vacuum) and then sectioned, followed by a second potting step and polishing. Fig. 2 shows a polished sample in topographic mode, and clearly indicates substantial sphere pull-out during polishing. It is also assumed that significantly more material was removed during sectioning. Hence, the interpretation of microstructures in this study can only be considered tentative due to the aforementioned microstructural damage caused by SEM sample preparation.

3. Results and discussion

Surface micrographs of the processed LSCF–coated Ag are shown in Fig. 3. The majority of the silver sphere surfaces

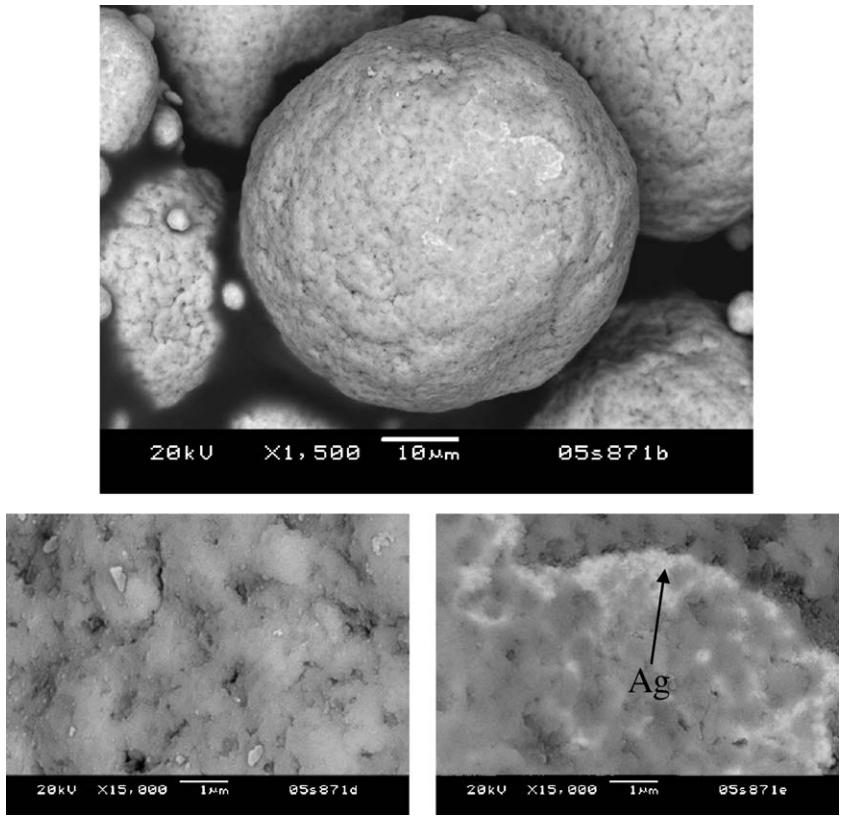

Fig. 3. Surface micrographs of silver spheres (44–53 μm) coated with LSCF-6428 predominantly indicating excellent coverage with small, discrete areas of poor coverage and silver exposure.

appeared to be well-coated, though regions of exposed surface were also observed. Fig. 4 shows cross-sections of the same material, and suggests excellent adherence between the silver host and LSCF coating (inset Fig. 4). It is also interesting to note that significantly smaller particles (retained fines in the commercially acquired silver spheres) can be equally well coated using this technique as shown in Fig. 5, which may of benefit in realizing higher power densities due to increased particle surface areas.

Fig. 6 shows 500 h performance data at 750 °C/0.7 V for three cells prepared using LSCF–coated Ag as a cathode. All of the cells indicated a very poor initial performance of <100 mW cm^{-2} but subsequently underwent significant conditioning to reach ~550–675 mW cm^{-2} in less than 100 h. Full cell electrochemical impedance spectroscopy (EIS) verified the conditioning of the cells. Fig. 7(a) and (b) indicate EIS data at 0 and 50 h, respectively. The data shows that the improved cell performance resulted from significant reductions in both

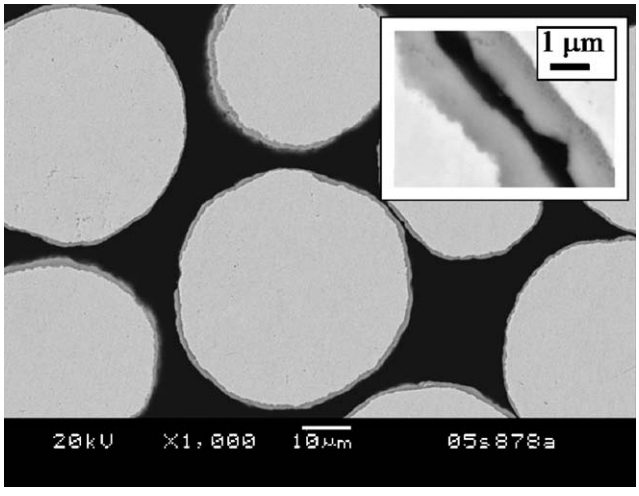

Fig. 4. Cross-sectional micrograph of silver spheres coated with LSCF-6428 predominantly indicating excellent coating adhesion.

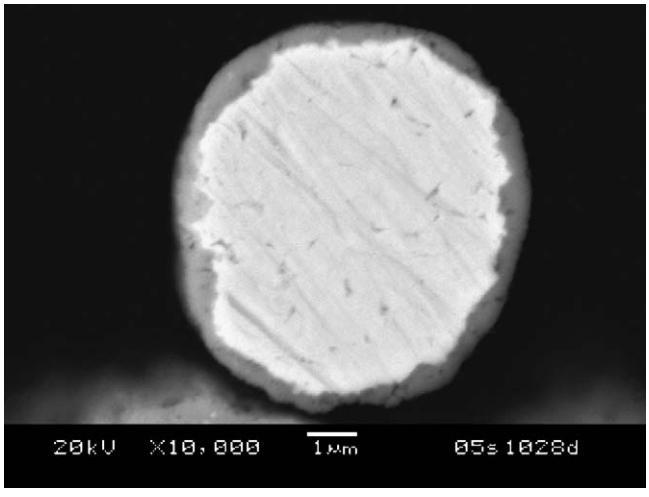

Fig. 5. Cross-sectional SEM showing the applicability of the mechanofusion process for coating smaller spheres.

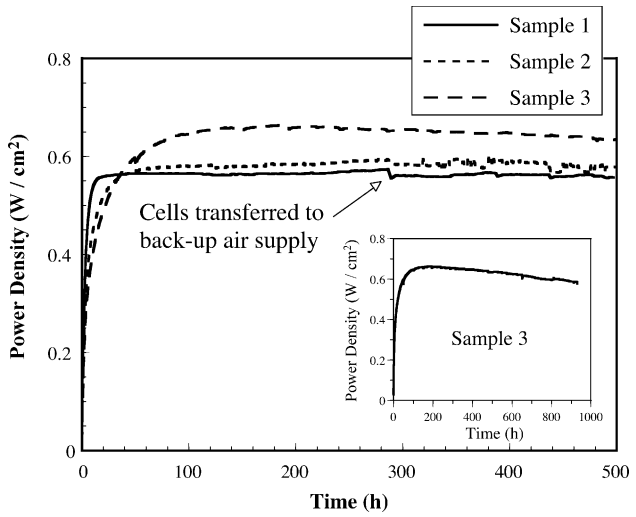

Fig. 6. 500 h performance data for anode-supported YSZ cells utilizing the Ag–LSCF composite cathode at 750 °C and 0.7 V.

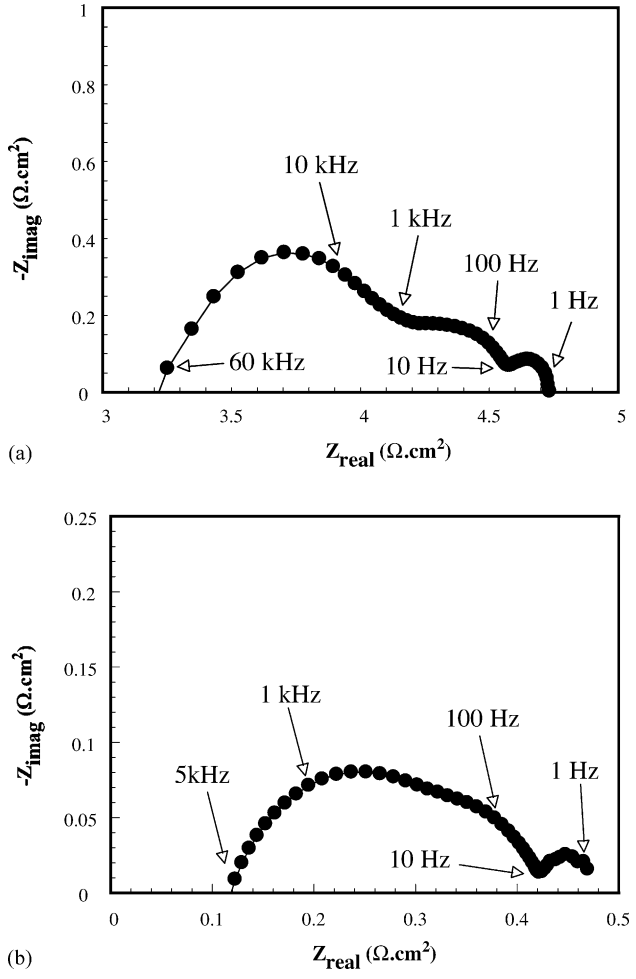

Fig. 7. (a) Impedance spectroscopy data at 750 °C prior to cathode conditioning. (b). Impedance spectroscopy data after 50 h of testing at 750 °C/0.7 V indicating significant cathode conditioning.

the ohmic and non-ohmic resistances. The former decreased by a factor of ∼25 and the latter by a factor of ∼4. SEM analysis was conducted on pre-tested (annealed at 800 °C/1 h under ∼10 psi compressive load and cooled to room temperature) and post-tested (annealed at 800 °C/1 h under ∼10 psi compressive load, cooled to 750 °C and tested at 0.7 V for 500 h) samples to establish potential changes in pre- and post-tested microstructures that might account for the conditioning characteristics of the Ag sphere-LSCF composite cathode. All samples indicated some diffusion of silver into the LSCF coating, as shown in Fig. 8. Interestingly, the silver appears to collect at the outer portion of the coating, and despite the diffusion of silver from the sphere surface the silver-LSCF interface remains remarkably intact, and free of porosity. It seems conceivable that the presence of sub-micron silver in the LSCF coating might provide enhanced catalytic activity for oxygen reduction, but since the silver also appeared in the pre-tested sample it fails to explain the observed performance conditioning. An additional observation is deformation of the spheres (under the compressive load) and presumably enhanced electrical contact, Fig. 9. However, once again both pre- and post-tested samples show this phenomenon, and as such it does not explain the performance conditioning.

SEM analysis did reveal two distinct microstructual changes with respect to pre- and post-tested samples. Firstly, Fig. 10 shows silver that has migrated into the SDC interlayer. This phenomenon has been previously observed in samples in which silver was used as the cathode current collector approximately 50 μm away from the cathode-electrolyte interface [16]. Secondly, Fig. 11 (and inset) indicates silver particles that have essentially wet (diffused along) the SDC interface forming intimate contact with the SDC interlayer. The presence of La, Sr, Fe and Co (detected by EDS) at the silver–SDC interface suggest that prior to testing the elongated particle was a coated LSCF sphere. It appears unlikely that the deformation of the sphere resulted from the compressive load applied at 750 °C since similar features were not observed in the pre-tested sample. It is perhaps conceivable that the discharge current results in electromigration (movement of ions under the influence of

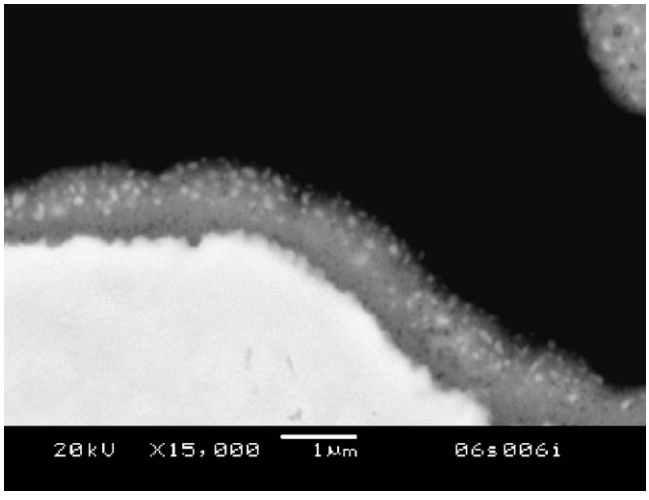

Fig. 8. Cross-sectional SEM showing diffusion of silver into the LSCF coating after annealing at 800 °C for 1 h.

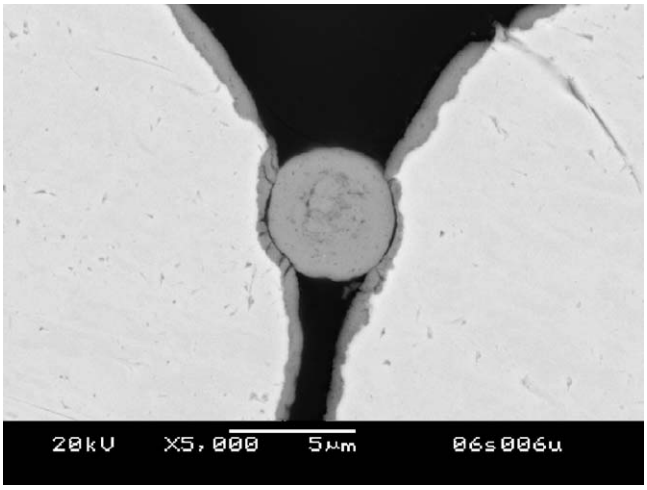

Fig. 9. Cross-sectional SEM indicating deformation of coated spheres and improved particle–particle contact.

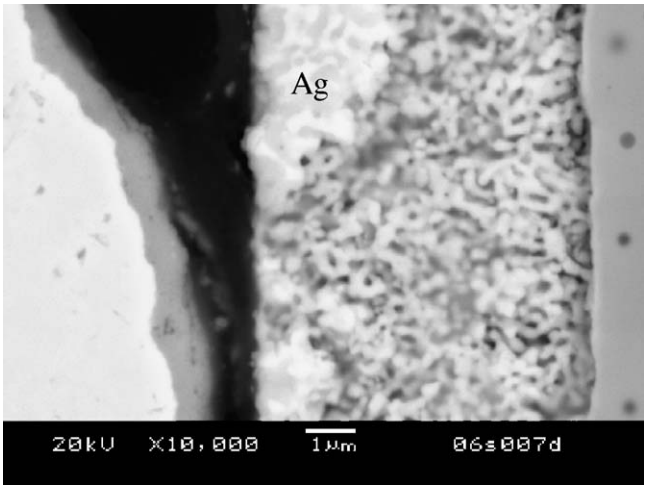

Fig. 10. Cross-sectional SEM indicating diffusion of silver into the porous SDC-20 interlayer.

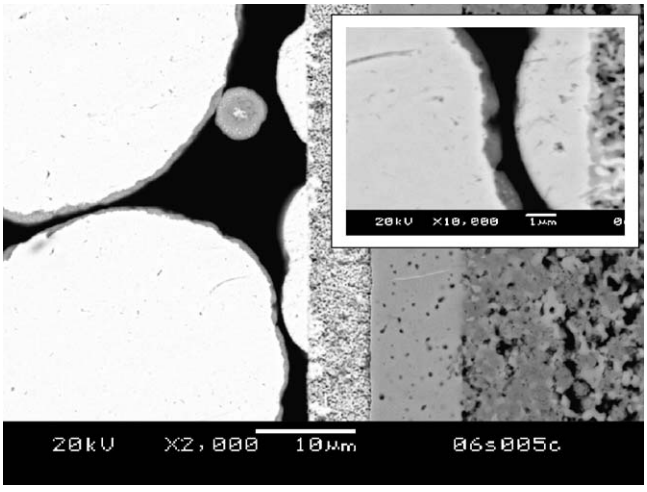

Fig. 11. Diffusion/spreading of silver (coated spheres) along the SDC surface during testing at 750 °C/0.7 V.

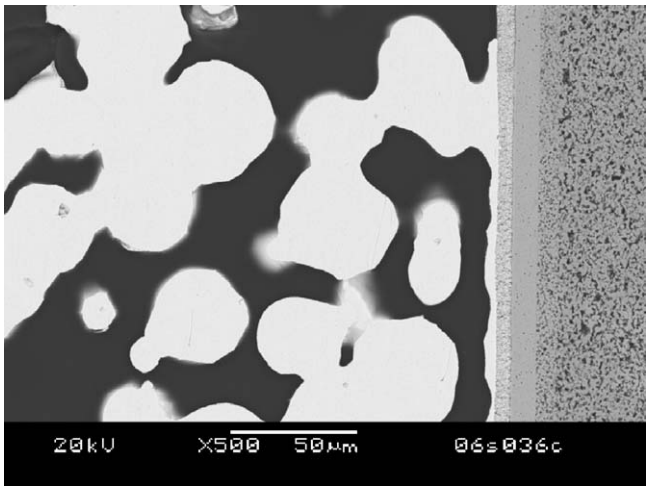

Fig. 12. Diffusion of silver (uncoated spheres) along the SDC surface during testing at 750 °C/0.7 V.

an electrical potential difference) of the silver, a phenomenon previously reported at 670–880 °C by Ho et al. [22]. Fig. 12 shows a cell tested with uncoated Ag spheres at 750 °C/0.7 V and also indicates a morphological change in the silver close to the SDC. The spheres are misshapen (not spherical) and in some areas silver extends long distances along the SDC surface, again possibly due to electromigration. To confirm the role of the discharge current in conditioning of these materials, a sample was subjected to intermittent testing whereby it was held at open circuit for 50 h periods with 5 min testing at 0.7 V between each open circuit hold. Fig. 13 indicates minimal change in performance for the intermittently tested cell over 200+ h (compared to the performance conditioning observed for continuously tested cells). In addition, SEM did not reveal the aforementioned silver wetting phenomenon for the intermittently tested cells. As such, it seems likely that the observed cell conditioning is associated with the diffusion (spreading) of the coated silver spheres across the SDC interface (under the influence of an electric field), and hence increased active cathode/electrolyte contact area.

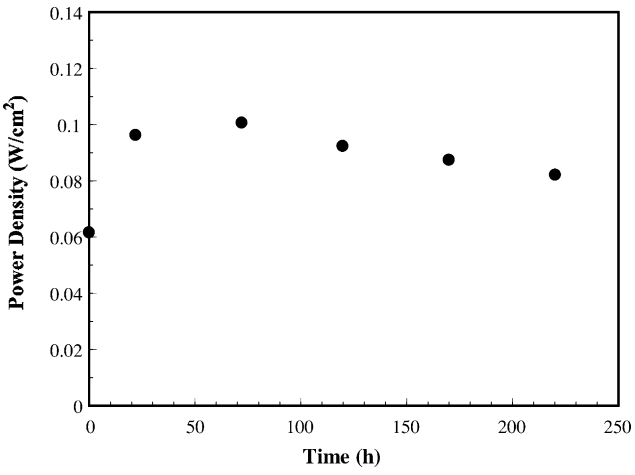

Fig. 13. 200+ h performance data for cell intermittently tested (50 h OCV, 5 min 0.7 V) at 750 °C.

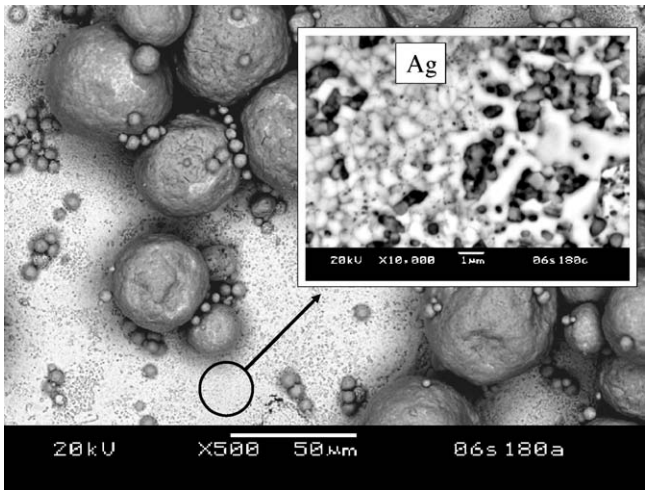

Fig. 14. SEM micrograph indicating excessive Ag diffusion across the SDC interlayer for a 750 °C test temperature.

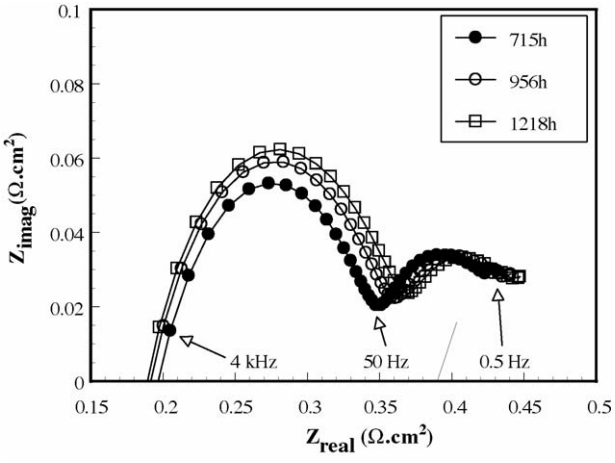

Fig. 16. Impedance spectroscopy data at 700 °C indicating slight performance degradation.

With respect to long-term stability of these materials at 750 °C, samples 1 and 2 (Fig. 6) indicate reasonable post-conditioning stability over a 500 h test period. Obviously, however, significantly longer test times are required to establish the true stability of the material, and indeed the data for sample 3, Fig. 6 inset (tested for 900+ h) indicates significant stability issues with a power degradation rate of 0.016%per hour from 200 to 900 h (at 0.7 V). SEM analysis of the SDC surface (with the cathode partially removed) reveals significant Ag diffusion across the entire SDC layer (Fig. 14). Hence, whilst some spreading/diffusion of the coated silver spheres across the electrolyte surface appears to be beneficial in extending the active electrolyte–cathode interface, continued diffusion of the silver likely reduces the triple phase boundary length and results in performance degradation.

Improved stability is, however, observed at 700 °C. Fig. 15 indicates >2000 h of data for a cell conditioned at 750 h for 50 h and then operated at 700 °C (conditioning at 700 °C takes considerably longer as shown in Fig. 15 inset). The cell exhibits continued conditioning up to 650–700 h, and then relatively stable performance. Degradation was, however, observed for this cell, and a drop of ∼4.9% in power density (at 0.7 V) was measured between 660 and 2270 h (∼3% power drop per 1000 h). Impedance data verifies the time-dependent degradation (Fig. 16), and interestingly it would appear that competing mechanisms are taking place. As the non-ohmic polarization above 50 Hz increases, the intercept with the real axis (ohmic resistance) decreases. Assignation of specific mechanisms to the observed changes in impedance response was not attempted in this study given the fact that the set-up does not incorporate a reference electrode, and as such prevents separation of electrochemical phenomena associated with the cathode or the anode. The validity (and limitations) of "full cell" impedance are discussed in a previous publication [16]. It should, however, be noted that previous work at PNNL using lanthanum manganite cathodes on identical anode-supported YSZ substrates indicated excellent stability during 2000 h of testing. As such it seems reasonable to conclude that the observed degradation in this study is not associated with the anode.

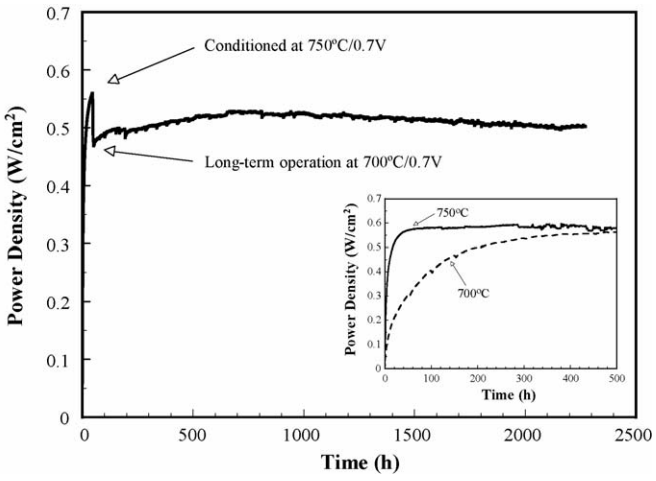

Fig. 15. 1500 h performance data for anode-supported YSZ cells utilizing the Ag–LSCF composite cathode at 700 °C and 0.7 V.

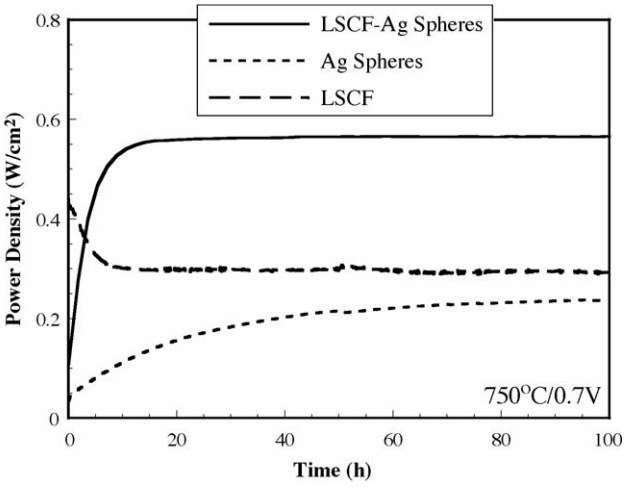

Fig. 17. 100 h performance of LSCF and uncoated Ag spheres compared to the Ag–LSCF composite.

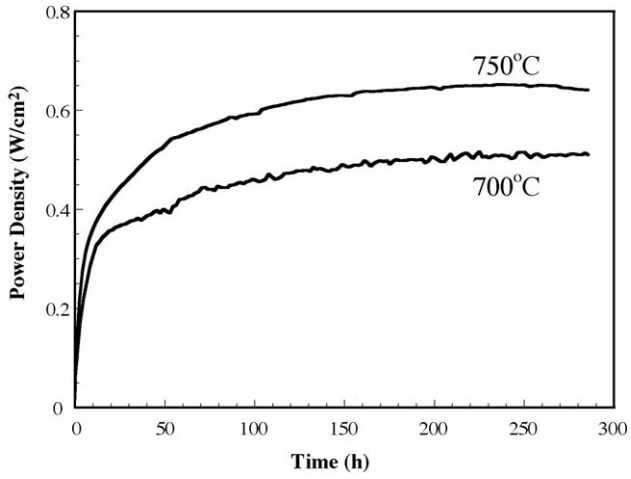

Fig. 18. 300 h performance data for anode-supported YSZ cells (without a protective ceria interlayer) utilizing the Ag–LSCF composite cathode at 750 °C and 0.7 V.

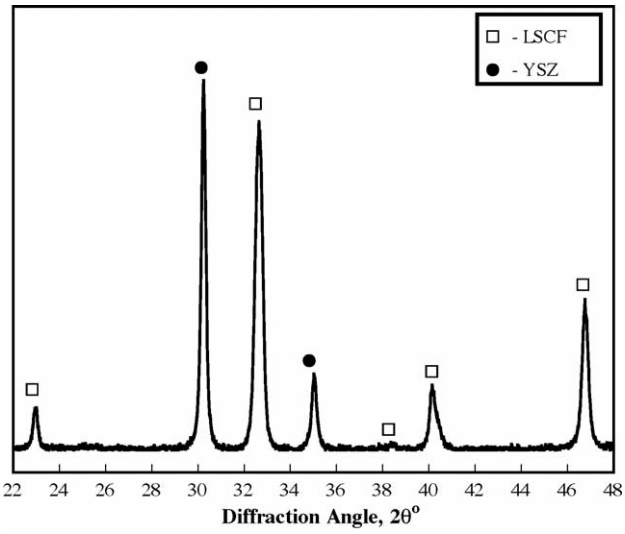

Fig. 19. Room temperature X-ray diffraction for an LSCF-6428/8-YSZ powder mixture reacted at 800 °C for 1 h. No Sr and/or La-zirconate phases are discernible.

Fig. 17 indicates 100 h performance data at 750 °C for the composite cathode as well as for cathodes consisting of either silver spheres or LSCF-6428 powder alone subjected to the same sintering temperature of 800 °C/1 h during cell heat-up. These tests were performed to confirm that the Ag–LSCF composite provided superior cathode performance when compared to each of its components tested alone. The LSCF cathode indicated reasonable initial performance (430 mW cm^{-2}) followed by rapid degradation (∼30% in 10 h), whilst the Ag sphere cathode exhibited very low initial power densities but underwent some degree of conditioning during the 100 h test period. Similar degradation characteristics for LSCF cathodes (operated around 750 °C) have been documented in a previous study [23].

Fig. 18 shows power density data (700–750 °C/0.7 V) for cells with the composite cathode, but without the protective SDC-20 interlayer. The maximum power densities achieved (within the indicated timeframe) were ∼650 and 500 mW cm^{-2}, at 750 and 700 °C, respectively. These results are promising in that they suggest that a protective ceria layer may not be required. This is substantiated by the lack of evidence of formation of La- and/or Sr-zirconate for an LSCF–YSZ powder mixture heated to 800 °C for 1 h, Fig. 19. However, additional confirmation (e.g. cross-sectional TEM) is required concerning possible reactivity or interdiffusion due to the detection limits of X-ray diffraction.

Two potential concerns exist concerning the ability to thermally cycle these materials. Firstly, there is a substantial CTE mismatch between the Ag-composite cathode (bulk CTE essentially equivalent to Ag: $\sim 20 \times 10^{-6}\,°C^{-1}$) and neighboring cell components (average CTE $\sim 12 \times 10^{-6}\,°C^{-1}$) though it is envisaged that the ductility of the silver may negate this concern. Secondly, a CTE mismatch also exists between LSCF ($\sim 17 \times 10^{-6}\,°C^{-1}$) and Ag ($\sim 20 \times 10^{-6}\,°C^{-1}$). Fig. 20 presents preliminary thermal cycling data. Each point represents a thermal cycle between 750 and 250 °C (at 3 °C min^{-1}) with a 1–2 h hold at each temperature for a total of 18 cycles. There is some indication of degradation over the first eight cycles though subsequent cycling indicates reasonable stability. With respect to sample integrity thermally cycling (even once) results in crack formation in the LSCF coating and silver diffusion into the cracks, Fig. 21. The effect of this microstructural change on long-term cell stability has not yet been established. One final factor worth consideration is cost. Based on a 10 liter batch the cost (raw materials and processing) of the coated Ag-spheres is approximately US$ 60 000 compared to US$ 25 000 for a typical perovskite cathode material. However, it should be noted that the use of these materials has the potential of removing two high temperature sintering steps. Firstly, the cathode is actually fired in situ during cell heat-up and sealing as opposed to a separate sintering step at temperatures >1000 °C. Secondly, initial data indicates that the SDC layer (and its associated and separate firing temperature of 1200 °C) may not be required since detrimental zirconate formation is avoided at the low cathode firing temperature (∼800 °C).

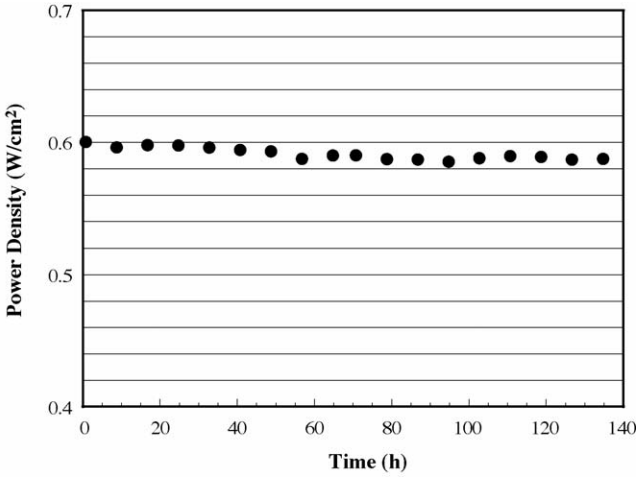

Fig. 20. Thermal cycling data for Ag–LSCF composite at 750 °C.

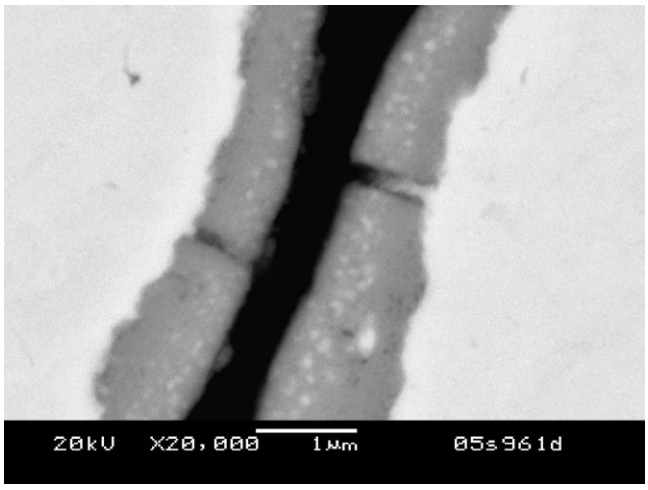

Fig. 21. Cracks in LSCF coating after thermal cycling between 200 and 800 °C.

4. Conclusion

Preliminary data suggests that silver spheres coated with LSCF powder (via a dry coating technique) provide reasonable power densities (>500 mW cm^{-2}) and surprising stability during >2000 h test duration at 700 °C and 0.7 V. The performance is characterized by initially low performance (>100 mW cm^{-2}) followed by substantial conditioning. Phenomena responsible for the conditioning characteristics of these materials have not been conclusively established though it appears that wetting (diffusion) of the coated spheres along the electrolyte surface may play a role by increasing the cathode–electrolyte contact area. Initial data looks promising though significantly more analysis is required to understand the conditioning mechanisms observed for this composite material, and to establish which of the composite materials plays the most significant role in performance conditioning and maximum power density. For example, is similar performance achievable for silver spheres coated in LSM, which is a considerably less active as an SOFC cathode compared to LSCF? In addition, it is necessary to investigate the "real-world" viability of these materials given the inherent problems of silver diffusivity and volatility.

Acknowledgements

Supported by the Solid-State Energy Conversion Alliance (SECA) Core Technology Program by the U.S. Department of Energy's National Energy Technology Laboratory (NETL). PNNL is operated by Battelle Memorial Institute for the U.S. Department of Energy under Contract DE-AC06-76RL. The authors are grateful to Nat Saenz and Shelley Carlson for SEM sample preparation.

References

[1] S.P. Simner, J.F. Bonnett, N.L. Canfield, K.D. Meinhardt, J.P. Shelton, V.L. Sprenkle, J.W. Stevenson, J. Power Sources 113 (2003) 1–10.
[2] S.P. Simner, J.F. Bonnett, N.L. Canfield, K.D. Meinhardt, J.P. Shelton, V.L. Sprenkle, J.W. Stevenson, Proceedings of the 2002 Fuel Cell Seminar on Fuel Cells—Reliable Clean Energy for the World, Palm Springs, CA, November 18–21, 2002, p. 344.
[3] K. Sasaki, J. Tamura, M. Dokiya, Solid State Ionics 144 (2001) 233–240.
[4] K. Sasaki, J. Tamura, H. Hosoda, T.N. Lan, K. Yasumoto, M. Dokiya, Solid State Ionics 148 (2002) 551–555.
[5] D. Simwonis, A. Naoumidis, F.J. Dias, J. Linke, A. Moropoulou, J. Mater. Res. 12 (1997) 1508–1518.
[6] L.S. Wang, S.A. Barnett, Solid State Ionics 76 (1995) 103–113.
[7] J.W. Erning, T. Hauber, U. Stimming, K. Wippermann, J. Power Sources 61 (1996) 205–211.
[8] S.P. Simner, M.D. Anderson, J.F. Bonnett, J.W. Stevenson, Proceedings of the 2003 Fuel Cell Seminar on Fuel Cells—Fuel Cells for Secure, Sustainable Energy, Miami Beach, FL, November 3–7, 2003, p. 388.
[9] M. Sahibzada, S.J. Benson, R.A. Rudkin, J.A. Kilner, Solid State Ionics 113–115 (1998) 285–290.
[10] S. Wang, T. Kato, S. Nagata, T. Honda, T. Kaneko, N. Iwashita, M. Dokiya, Solid State Ionics 146 (2002) 203–210.
[11] S. Wang, T. Kato, S. Nagata, T. Kaneko, N. Iwashita, T. Honda, M. Dokiya, Solid State Ionics 152–153 (2002) 477–484.
[12] M. Watanabe, H. Uchida, M. Shibata, N. Mochizuki, K. Amikura, J. Electrochem. Soc. 141 (1994) 342–345.
[13] H. Uchida, M. Yoshida, M. Watanabe, J. Electrochem. Soc. 146 (1999) 1–7.
[14] H. Uchida, S. Arisaka, M. Watanabe, Solid State Ionics 135 (2000) 347–351.
[15] V.A.C. Haanappel, D. Rutenbeck, A. Mai, S. Uhlenbruck, D. Sebold, H. Wesemeyer, B. Rowekamp, C. Tropartz, F. Tietz, J. Power Sources 130 (2004) 119–128.
[16] S.P. Simner, M.D. Anderson, L.R. Pederson, J.W. Stevenson, J. Electrochem. Soc. 152 (2005) 1851–1859.
[17] R. Pfeffer, R.N. Dave, D. Wei, M. Ramlakhan, Powder Technol. 117 (2001) 40–67.
[18] T. Iwasaki, m. Satoh, T. Ito, J. Mater. Proc. Technol. 146 (2004) 330–337.
[19] T. Fukui, K. Murata, S. Ohara, H. Abe, M. Naito, K. Nogi, J. Power Sources 125 (2004) 17–21.
[20] T. Fukui, S. Ohara, H. Okawa, M. Naito, K. Nogi, J. Eur. Ceram. Soc. 23 (2003) 2835–2840.
[21] S.P. Simner, M.D. Anderson, G.-G. Xia, Z. Yang, L.R. Pederson, J.W. Stevenson, J. Electrochem. Soc. 152 (2005) 740–745.
[22] P.S. Ho, H.B. Huntington, J. Phys. Chem. Solids 27 (1966) 1319–1329.
[23] A. Mai, V.A.C. Haanappel, S. Uhlenbruck, F. Tietz, D. Stöver, Solid State Ionics 176 (2005) 1341–1350.